Bonding to dentin using an experimental zirconium oxynitrate etchant

# Bonding to dentin using an experimental zirconium oxynitrate etchant

**Edoardo Mancuso[1], Allegra Comba[1], Claudia Mazzitelli[1], Tatjana Maravic[1], Uros Josic[1], Federico Del Bianco[1], Franklin R Tay[2], Lorenzo Breschi[1], Annalisa Mazzoni[1]**

[1]Department of Biomedical and Neuromotor Sciences, DIBINEM, University of Bologna - Alma Mater Studiorum, Via San Vitale 59, 40125 Bologna, Italy;

[2]Department of Endodontics, The Dental College of Georgia, Augusta University, 1430 John Wesley Gilbert Drive, Augusta, GA 30912, USA.

**Keywords:** adhesive; dentin etchant; longevity; MMP inhibition; zirconium oxynitrate**;** zymography

**Acknowledgements:** The present study was partially supported by Ivoclar Vivadent.

**Corresponding author:** Prof. Lorenzo Breschi, Department of Biomedical and Neuromotor Sciences, DIBINEM, University of Bologna - Alma Mater Studiorum, Via San Vitale 59, 40125, Bologna, Italy, Tel: +39-051-2088139; Fax: +39-051-225208; email: lorenzo.breschi@unibo.it

**Bonding to dentin using an experimental zirconium oxynitrate etchant**

**Abstract**

**Objective:** To investigate, by means of microtensile bond strength test (μTBS), nanoleakage expression analysis (NL), gelatin zymography and in situ zymography, the effects of an experimental metal salt-based zirconium oxynitrate etchant [ZrO(NO3)2,] – ZON with two simplified adhesives on long-term bond strength and endogenous enzymatic activities.

Methods: Middle/deep coronal dentin surfaces (N=32) were conditioned either with a traditional 37% H3PO4 etchant (TE) or with ZON. Further, a single-component etch-and-rinse adhesive (EF) or a universal adhesive (AU) were applied and μTBS and NL tests were performed. Additional freshly extracted teeth were processed for gelatin zymography and in situ zymography evaluation. The tests were performed at baseline and (T0) and after 1-year-aging (T12). Bond strength and in situ zymography results were analyzed using analysis of variance (ANOVA) (three-way and one-way, respectively), while Chi-squared test was used for the NL results. Statistical significance was preset at $\alpha$=0.05.

Results: All the investigated factors (adhesive system, dentin conditioner and aging) significantly influenced μTBS, with the AU and ZON performing better compared to EF and TE, respectively, and with lower bond strength values after aging ($p<0.05$). Incremented silver nitrate deposits were observed at the adhesive interfaces after aging, especially for the TE groups ($p<0.05$). Further, the experimental groups treated with ZON had significantly lower levels of enzymatic activity compared to TE, as shown by gelatin and in situ zymography ($p<0.05$).

Conclusions: The experimental etchant demonstrated promising results in hybrid-layer preservation over time when used with simplified bonding systems, and could therefore be recommended in the clinical practice.

## 1. Introduction

Adhesion to dentin has been a challenge for researchers and clinicians ever since dentin bonding became ~~becomes~~ a clinical procedure. This is attributed to the structural complexity of the dentin substrate. Attributes such as the intrinsic wetness of deep vital dentin [1], heterogeneity of its intrinsic constituents [2] and the sensitivity of the organic matrix to operator manipulation [1] renders bonding to dentin extremely taxing to be performed well.

~~In the grand scheme of things, dentin bonding may be perceived as a form of tissue engineering [2].~~ Different clinical steps are used to "condition" and "prime" the tooth substrate. These steps enable a clinician to create dentin surface conditions that are conducive to receiving a methacrylate resin-based adhesive. Errors can occur during these clinical steps [2–4]. ~~In addition, physical and chemical problems may occur in the resin-dentin interface after bonding. Problems such as hydrolysis of the functional resin monomers, plasticization of the incompletely polymerized resin matrix and degradation of the incomplete resin-infiltrated collagen matrix [2,3] contribute to premature deterioration of the adhesive seal [3,4].~~ The adhesion process begins with conditioning of the dentin surface with an acid etchant or a solution of acidic resin monomers to create a layer of partially-demineralized or fully-demineralized collagen-rich organic matrix for infiltration of adhesive resin. During this process ~~Ideally, the adhesive resin should fully infiltrate the collagen fibrils, envelope and interact with the fibrils to form a stable hybrid layer. However more often than not,~~ a water-rich, resin-sparse zone ~~is~~ might be produced at the base of the hybrid layer. This zone contains denuded collagen fibrils that are surrounded by water molecules of dental origin [5,6]. Many studies have reported that this ~~water-rich, resin-sparse~~ zone is susceptible to degradation by host-derived matrix metalloproteinases (MMPs) [7,8] and cysteine cathepsins [9]. Following degradation, the longevity of resin-dentin bonds is undermined [5,10]. Despite attempts to improve adhesive performance and to promote more stable resin-dentin interfaces through the use of protease inhibitors, degradation of these interfaces have been reported with all types of bonding approaches [2, 5, 6].

Therapeutic systems, blended to an adhesive or used as primer in a separate step, have been used to prevent the degradation of the resin-dentin interface mediated by MMPs [5,11,12]. Phosphoric acid etchants containing MMP inhibitors have also been developed [11]. ~~Apart from etching dental tissues, some of these etchants may be used on restoration materials such as ceramics or zirconia [14].~~ An experimental zirconium oxynitrate conditioner [$ZrO(NO_3)_2$] has recently been introduced to adhesive dentistry. Zirconium oxynitrate has only been used previously in applied chemistry or as a radiopacifying material in endodontic cements [12]. Promising results have recently been reported when $ZrO(NO_3)_2$ was used as an enamel etchant, in combination with different adhesive systems [11]. Introduction of an etching product that can dissolve the inorganic component of dentin, reduce nanoleakage and inhibit MMP-mediated proteolytic activity at the resin-dentin interface is highly desirable to maintain bond stability over time [9].

~~Single-component universal adhesives are the latest category of simplified adhesive systems. They were introduced to simplify the clinical procedures involved in dentin bonding and to reduce operator mismanagement to the minimum. Despite their much acclaimed versatility in offering a clinician the option in using the adhesive in the self-etch mode, etch-and-rinse mode or selective enamel etching mode, there have been concerns whether these adhesives really improve long-term bonding performanc [15]. When applied in the etch-and-rinse mode, resin-sparse, water-rich domains were observed on the adhesive interface that were similar to other categories of etch-and-rinse adhesives, with premature degradation of resin-dentin bonds that are similar to those identified from previous adhesive generations [16]. Nevertheless, improvements in dentin adhesion strength and maintenance of bond stability over time have been reported when universal adhesives were used with therapeutic primers [2, 5, 12].~~

Capitalizing on the aforementioned considerations, the objectives of the present *in vitro* study were to evaluate the immediate ($T_0$) *vs* 1 year ($T_{12}$) microtensile bond strength to dentin, interfacial nanoleakage expression and the effects of endogenous enzymatic activity on hybrid layers created by

two simplified adhesive systems (one single-component etch-and-rinse ~~2-step~~ adhesive and one universal adhesive). These adhesives were applied to dentin after the latter was conditioned with a $H_3PO_4$ acid etchant or an experimental $ZrO(NO_3)_2$ etchant. The null hypothesis tested were that the experimental $ZrO(NO_3)_2$ etchant: 1) has no effect on the immediate bonding performance of the tested adhesives to dentin; 2) has no effect on the maintenance of bonding performance after laboratory aging; and 3) has no effect on inhibiting endogenous dentin MMPs activity immediately or over time**.**

## 2. Material and methods

### 2.1. Microtensile bond strength test (μTBS)

Sixty-four freshly extracted non-carious human third molars were obtained from anonymous individuals following their informed consent. The project protocol was approved by the Ethical Committee (protocol N°: 71/2019/OSS/AUSLBO, approved on 23/01/2019).

Tooth crowns were removed with a low-speed diamond saw under water cooling (Microremet, Remet, Bologna, Italy) to expose deep coronal dentin. Cut dentin surfaces were examined with a stereoscopical microscope to ensure that they were devoid of enamel remnants. A standardized smear layer was created on each dentin surface using 600-grit wet silicon carbide paper and water lubrication. Dentin conditioning was performed with 37% $H_3PO_4$ – TE (Total Etch ~~(TE)~~; Ivoclar Vivadent, Schaan, Liechtenstein) or an experimental zirconium oxynitrate gel (ZON) (Ivoclar Vivadent). After dentin etching, a universal adhesi – AU (Adhese Universal ~~(AU)~~; Ivoclar Vivadent) was used in the etch-and-rinse mode. Alternatively, a single-component etch-and-rinse adhesive – EF ~~2-step self-etch adhesive~~ (Excite F ~~(EF)~~; Ivoclar Vivadent) was used in the etch-and-rinse ~~self-etch~~ mode. This resulted in the establishment of 4 experimental groups (n = 16): 1) ZON + AU; 2) TE + AU; 3) ZON + EF; 4) TE + EF. The chemical composition of the adhesives and etchants and their instructions for use are shown in Table 1.

After polymerization of the respective adhesive, a 4 mm-thick layer of composite build-up was performed with a nanohybrid resin composite (Tetric Evo Ceram Bulk Fill, Ivoclar Vivadent).

Light curing was performed for 20 s with a light-emitting diode curing light (DemiPlus; Kerr Corp., Orange, CA, USA) with an output of 500 mW/cm².

The bonded specimens were serially sectioned to obtain beams with ~0.9 mm × ~0.9 mm cross-sectional area, in accordance with the non-trimming technique of the microtensile test. Bond testing was performed after the beams were aged in artificial saliva at 37 °C for 24 h ($T_0$) or 1 year ($T_{12}$). The exact dimension of each beam was measured using a pair of digital calipers. Each beam was stressed under tension to failure using a simplified bond testing machine (Shear Bond Tester; Bisco, Schaumburg, IL, USA) at a crosshead speed of 1 mm/min. The number of prematurely debonded beams in each experimental group was recorded. Null bond strength values were not included in the statistical analysis because the number of prematurely debonded beams did not exceed 3% of the total number of tested specimens and were similarly distributed within the groups. A single observer evaluated each side of the fractured sticks with a stereomicroscope at 50× ~~optical microscopy at 50×~~ magnification to determine the mode of failure. Failure was classified as adhesive (A), cohesive in dentin (CD), cohesive in composite (CC) or mixed failure (M).

### 2.2. Nanoleakage expression

Four additional teeth per group were sectioned into 1 mm-thick slices of mid-coronal dentin and bonded in the manner described for the μTBS test. After bonding, 1 mm-thick resin composite build-ups were made using TetricEvo Flow (Ivoclar Vivadent). The specimens were sectioned vertically into 1-mm thick beams to expose the bonding surfaces. Half of the beams were stored in the artificial saliva at 37 °C for 24 h ($T_0$). The remaining half was stored the artificial saliva for 12 months ($T_{12}$). After aging, the specimens were immersed in 50 wt% ammoniacal $AgNO_3$ solution for 24 h, following the protocol described by Tay *et al.* [13]. The silver tracer infiltrated specimens were thoroughly rinsed with distilled water and immersed in a photo-developing solution for 8 h under a fluorescent light to reduce silver ions that infiltrated voids along the bonded interfaces into metallic silver grains.

Each specimen was fixed to a glass slab and polished with a polishing device (LS2; Remet) under water irrigation. Polishing was performed using a series of silicon carbide papers with increasing fineness (180-, 600-, 1200-, 2400-, and 4000-grit). Observations were made using a light microscope (E800; Nikon, Tokyo, Japan). Images of the resin-dentin interfaces were obtained at 20x magnification. The severity of interfacial nanoleakage was quantified using a four-point scale by one experienced investigator. Scoring was performed using the method described by Saboia *et al.* [14] with the scores representing the percentage distribution of silver deposits within the resin-dentin interfaces.

### 2.3 Gelatin zymography

Zymography was performed using the method reported by Mazzoni *et al.* [15]. Briefly, mineralized dentin powder was obtained from eight extracted human third molars. Each tooth was ground free of enamel and cementum; pulpal soft tissue was removed with excavators and hand files. Dentin powder was obtained by freezing dentin chips in liquid nitrogen and triturating them in a ball mill (Retsch Mill; Reimiller, Reggio Emilia, Italy). ~~Retsch mill (Reimiller, Reggio Emilia, Italy)~~. The mineralized dentin powder was pooled, sieved, dried and kept frozen until use. Aliquots of mineralized dentin powder were divided into 3 groups:

- Mineralized dentin control (C);
- Dentin powder demineralized with ZON for 10 min (ZON);
- Dentin powder demineralized with TE for 10 min (TE).

In the groups treated with a liquid etchant, the acid was neutralized after 10 min and centrifuged. The supernatant was removed and the powder was rinsed 2 more times with distilled water and re-centrifuged for 20 min at 4 °C. For protein extraction, dentin powder aliquots were re-suspended in extraction buffer (50 mM Tris–HCl, pH 6, containing 5 mM $CaCl_2$, 100 mM NaCl, 0.1% Triton X-100, 0.1% nonionic detergent P-40, 0.1 mM $ZnCl_2$ and 0.02% $NaN_3$) for 24 h at 4 °C. The dentin powder-containing buffers were intermittently sonicated for 10 min and centrifuged for 20 min at 4

°C. The supernatants were discarded and re-centrifuged. The extracted proteins were concentrated using Vivaspin centrifugal concentrator (10 kDa molecular weight cut-off; Vivaspin Sartorius Stedim Biotech, Goettingen, Germany) for 30 min at 25 °C (15 G × 3 times). Total protein concentration in the dentin extracts was determined using the Bradford assay (Bio-Rad Bradford Protein Assay; Bio-Rad, Hercules, CA, USA). Dentin proteins aliquots (60 µg each) were diluted in Laemmli sample buffer in a 4:1 ratio and subjected to electrophoresis under non-reducing conditions in 10% sodium dodecyl sulfate-polyacrylamide gel electrophoresis (SDS-PAGE) containing 1 mg/mL fluorescein-labeled gelatin. Pre-stained, low-range molecular weight SDS-PAGE standards (Bio-Rad) were used as molecular-weight markers. After electrophoresis, the gels were washed for 1 h in 2% Triton X-100 and incubated in zymography activation buffer (50 mmol/L Tris–HCl, 5 mmol/L $CaCl_2$, pH 7.4) for 48 h. Proteolytic activity was evaluated using an ultraviolet light scanner (ChemiDoc Universal Hood, Bio-Rad). Gelatinase activities in the extracts were analyzed in duplicate. Images were qualitatively examined and gelatinase activities were quantified using an image processing software ~~ImageJ software~~ (ImageJ; National Institute of Health, Bethesda, MD, USA).

### 2.4. *In situ* zymography of resin-dentin interfaces

One millimeter-thick slabs of middle/deep coronal dentin were obtained from three extracted human third molars using a low-speed saw (Micromet) with water-cooling. Two dentin slabs were obtained from each tooth. Each slab was further divided into 2 pieces, so that testing of the four experimental groups was performed using the same dentin substrate. A standardized smear layer was created on each dentin surface using 600-grit silicon carbide paper under water cooling. The specimens were then randomly assigned to the same 4 groups (n = 3) described for µTBS. Identical bonding procedures were performed as previously described. Each bonded specimen was light-cured for 20 s using a light emission diode light-curing unit (Demi Plus). Resin-dentin interfaces were exposed by cutting the bonded specimens vertically into 1 mm-thick sticks using the slow-speed saw under water cooling. The sticks were affixed to glass slides with cyanoacrylate glue, and polished to

obtain ~50 μm-thick slabs using a series of wet silicon carbide papers. Self-quenched fluorescein-conjugated gelatin was used as the MMP substrate (E-12055, Molecular Probes, Eugene, OR, USA) for *in situ* zymography at the baseline ($T_0$) and after 12 months ($T_{12}$) of storage in artificial saliva at 37 °C, as previously described [16]. The fluorescent gelatin mixture was placed on top of each slab and covered with a glass coverslip. The slides were incubated in a humidified chamber at 37 °C overnight. During incubation, the assemblies were prevented from direct contact with water and were protected from exposure to light. After incubation, the microscopic slides were examined using a confocal laser scanning microscope (excitation wavelength 488 nm; emission wavelength 530 nm; Model A1-R; Nikon, Tokyo, Japan). For each specimen, a series of images were made to visualize hydrolysis of the quenched fluorescein-conjugated gelatin substrate as an indicator of endogenous gelatinolytic activity. Enzymatic activity was quantified as the integrated density of the fluorescence signals using ImageJ software.

### 2.5 Statistical analyses

Data sets obtained from bond strength testing, nanoleakage evaluation and *in situ* zymography were first validated individually for their normality (Shapiro-Wilk test) and homoscedasticity assumptions (modified Levene test) prior to the use of parametric statistical methods for analysis. Three independent variables were involved in μTBS testing: adhesive systems, dentin conditioners and aging time. Accordingly, a three-factor analysis of variance (ANOVA) was performed to identify the effects of the three independent variables on bond strength. Post-hoc pairwise comparisons were conducted using the Tukey test. The nanoleakage results were analyzed using Chi-squared test. Data derived from *in situ* zymography were analyzed with one-factor ANOVA and post-hoc Tukey test. All analyses were performed using a statistical software ~~Stata v.12.0. software~~ (Stata v.12.0.; StataCorp LLC, College Station, TX, USA). For all analyses, statistical significance was preset at $\alpha = 0.05$.

## 3. Results

### 3.1. Microtensile bond strength test (μTBS)

Bond strength values at $T_0$ and $T_{12}$ are depicted in Table 2. Three-way ANOVA test showed that all the investigated factors (adhesive systems, dentin conditioners and aging), significantly influenced bond strength results ($p < 0.05$). In addition, significant interactions were identified between adhesive systems and dentin conditioners ($p < 0.05$) and between adhesive systems and aging ($p < 0.05$). At $T_0$, ZON/AU had the highest mean bond strength among the tested groups ($p < 0.05$). No differences were observed among TE/AU, ZON/EF and TE/EF.

Significant difference in bond strength was observed after laboratory aging ($p < 0.05$). Pairwise comparisons indicated that bond strength values after aging were in the order: ZON/AU = TE/AU > TE/AU = ZON/EF > ZON/EF = TE/EF ($p < 0.05$). Compared with the immediate bond strength results, bond strength significantly declined for all groups ($p < 0.05$) after laboratory aging except for TE/AU.

Table 3 summarizes the percentage distribution of different failure modes identified after μTBS test at $T_0$ and $T_{12}$. Whereas at $T_0$ for all groups but TE/AU the majority of the failures were adhesive, followed by mixed failures and cohesive in resin composite, at $T_{12}$, there were less mixed fractures and, especially in the AU groups, more cohesive failure in resin composite, irrespective of the dentin conditioner employed. After aging in the ZON/EF group there an increment in the adhesive failures.

### 3.2. Nanoleakage expression

Interfacial nanoleakage scores are summarized in Figure 1. Representative light microscopy images of nanoleakage expression for the four experimental groups tested at $T_0$ or $T_{12}$ are shown in Figure 2 and Figure 3, respectively. The Chi-squared test indicated differences among the experimental groups in the percentage of silver deposition along the resin-dentin interfaces. At $T_0$, there was no difference in nanoleakage expression among the experimental groups. There were more extensive silver deposits along the resin-dentin interfaces after the specimens were aged for 12 months ($T_{12}$), compared with $T_0$ ($p < 0.05$) and this manifestation was independent of the tested group.

When the etchants were compared, the two groups that were etched with TE had more extensive interfacial silver deposits compared to the ZON groups ($p < 0.05$).

### 3.3 Gelatin zymography

Zymography results are shown in Figure 4A and Figure 4B~~5~~. Qualitative and quantitative zymography assays identified the proform and active form of MMP-9 (≈92 kDa and 86 kDa, respectively) in mineralized dentin. Expression of MMP-9 was more pronounced in dentin demineralized with TE. In addition, an extra band that corresponded to the molecular weight of active MMP-2 was observed at ≈66 kDa. Dentin demineralized with ZON showed bands that corresponded to the molecular weight of pro-MMP-9, the intensity of which was slightly lower that what was presented in the TE-demineralized dentin. There was complete inhibition of MMP-2 and MMP-9 active forms.

### 3.4 *In situ* zymography of resin-dentin interfaces

Qualitative and quantitative *in situ* zymography results are shown in Figures 5-7 ~~6–8~~. The green fluorescence signals identified from the AU groups at $T_0$ and $T_{12}$ were lower compared to those exhibited by the EF groups. All groups demonstrated the general tendency of augmented protease activity after aging. Statistical analysis indicated that experimental groups treated with ZON had significantly lower levels of fluorescence at $T_0$, compared to TE, irrespective of the bonding system employed ($p < 0.05$). After aging, there was also less fluorescence for ZON-etched dentin for the AU adhesive ($p < 0.05$). However, fluorescence in the ZON-etched dentin and TE-etched dentin that were bonded with the EF self-etch adhesive were very high and there was no difference between these two groups at $T_{12}$ (Figure ~~8~~ 7, 3$^{rd}$ and 4$^{th}$ green columns; $p > 0.05$).

## 4. Discussion

The first null hypothesis that "the experimental $ZrO(NO_3)_2$ etchant has no effect on the immediate bonding performance of the tested adhesives to dentin" has to be rejected because the experimental ZON etchant not only did not impair immediate bond strength, but increased that of the

universal adhesive AU. There were significant reductions in the bond strength values after 1 year of laboratory aging for all groups except TE/AU. Accordingly, the second null hypothesis that "the experimental $ZrO(NO_3)_2$ etchant has no effect on the maintenance of bonding performance after laboratory aging" cannot be rejected. Compared with phosphoric acid etching (i.e. TE groups), etching with ZON decreased the activity of MMPs in the hybrid layer immediately irrespective of the adhesive employed. After aging, there was also significantly less MMPs activity in ZON-etched dentin for the AU adhesive. However, there was no difference between the MMP activity exhibited by the two EF ~~self-etch~~ adhesive bonded groups at $T_{12}$. Hence the third null hypothesis that "the experimental $ZrO(NO_3)_2$ etchant has no effect on inhibiting endogenous dentin MMP activity immediately or over time" can only be partially rejected.

An experimental therapeutic etching agent $ZrO(NO_3)_2$ was used for etching dentin in the present study prior to adhesive application. This etchant previously demonstrated promising bonding results and stable bonds after thermocycling when used with different adhesives on enamel [11]. To date, no information is available on the effects of the experimental etchant on the bonding performance of simplified adhesive systems to dentin.

The manufacturer claimed that the experimental $ZrO(NO_3)_2$ etchant has a self-limiting etching capacity. This should prevent the ZON etchant from over-demineralizing dentin unnecessarily within the time of application on the dentin surface. The ZON etchant is a Lewis acidic metal salt that is readily soluble in water. Water is necessary for the dissolution of the zirconium salt to create an acidic condition (pH = 0.56) that is conducive for demineralizing the inorganic components of dentin. During demineralization, $Ca^{2+}$ and $PO_4^{2-}$ ions are released from dentin and these ions bind to the $Zr^{4+}$ ions as to form a solid complex [17]. A preliminary scanning electron microscopy and energy-dispersive X-ray spectroscopy study performed by this research group confirmed the precipitation of $Ca^{2+}$ and $P^{3-}$ ions on the surface of dentin treated with ZON for 30 s, with tubules more closed compared to dentin etched with TE for 15 s (unpublished data). Studies are ongoing to reaffirm this

hypothesis and furnish ulterior information on the etching and self-limiting mechanism of the experimental material. ~~Because of the limited information available, the authors could only speculate that the purported self-limiting etching capacity of the experimental etchant is attributed to the sedimentation of the $Ca^{2+}$ - Zr and $P^{+}$ - Zr complexes at the base of the demineralized collagen matrix. This hypothesis needs to be confirmed in future studies.~~

The ZON etchant increased the immediate bond strength of AU to dentin, resulting in acceptable immediate adhesion in all the experimental groups (Table 2). It has been speculated cautiously that the chemical interaction between dentin and MDP does not have any influence on the immediate bond strength to dentin, but helps to improve bond stability [18]. Such a speculation was validated in the present study, wherein the bond strength of AU ~~increased~~ did not decrease with the use of conventional etching after 12 months of laboratory aging (Table 2). Significant decrease in bond strength was observed for ZON/AU at $T_{12}$, however, it is possible that the bond strength values in this group were underestimated, since the adhesive bond strength between the tooth and the composite exceeded the cohesive bond strength within the material itself (73% of CC failure mode). ~~*In situ* zymography identified more potent inhibition of ZON enzymatic activity by ZON, when compared with TE, at $T_0$ and $T_{12}$ (Figure 8).~~ The 10-MDP and the methacrylated carboxylic acid polymer incorporated within AU possibly enabled the adhesive to produce durable bonds to dentin [19,20]. Nurrohman *et al.* [21] investigated the interaction of MDP and the carboxylic-based functional co-polymer on the formation of crystallites on the bottom of the hybrid layer and preservation of the underlying dentin structure after the exposure to acid attack. Interestingly, the study revealed that both functional monomers/polymers were more efficient in creating a crystallite layer and protecting the underlying dentin structure in the self-etch compared to etch-and-rinse systems, since the etching with phosphoric acid always penetrates deeper into the dentin structure than the adhesive resin itself [2]. Although in the control MDP-containing etch-and-rinse samples there was apatite formation on the bottom of the hybrid layer, after the acid attack, the destruction of the underlying dentin structure was prevented by the MDP only partially. AU in general performed better in the present study in

terms of bond strength. AU contains both the 10-MDP and methacrylated carboxylic acid polymer, contributing to a possibly stronger interaction with the apatite crystals on the bottom of the etched dentin surface, leading to higher bond strength compared to EF, even after aging in the artificial saliva. Furthermore, the precipitation of $Ca^{2+}$ and $PO4^{2-}$ ions on the bottom of the hybrid layer formed after etching with ZON might have enhanced the MDP interaction with the apatite crystals.

~~Creation of nano-layering at the adhesive interface and the deposition of more stable MDP-Ca salt were claimed by some authors for the creation of reliable MDP-based bonding [22].~~ The zymography results in the present work revealed inhibition of MMP activities when the ZON etchant was used to demineralize the dentin surface, a feature that was not identified with the use of the TE etchant. *In situ* zymography identified more potent inhibition of enzymatic activity by ZON, when compared with TE, at $T_0$ and $T_{12}$ (Figure 7 ~~8~~). These results could be explained by the ability of ZON to bind to $Ca^{2+}$ ions via chelation. Because of this mechanism, the ZON etchant removes $Ca^{2+}$ ions from the catalytic site of MMP-2 and MMP-9 that are crucial for the optimal function of these proteases [19]. Such a phenomenon is analogous to the chelation effect of EDTA in MMPs inhibition [20]. Further studies should be performed to validate the depth of demineralization created by the ZON etchant on dentin.

The 2-step self-etch adhesive EF generated the lowest bond strengths among the four experimental groups, both at $T_0$ and $T_{12}$, irrespective of etching dentin with TE or ZON. Bond strength decreased after one year of artificial aging (Table 2). Although ZON/EF showed the lowest enzymatic activity among all $T_0$ groups, after 1 year of artificial aging the enzymatic activity of this group was comparable to aged TE/EF (Figure 8). The higher presence of ~~HEMA and~~ Bis-GMA, a hydrophobic resin ~~functional~~ monomer, in the formulation of EF compared to AU probably accounted for poorer hybridization of the adhesive resin blend ~~drawing water from dentinal tubules from the underlying perfused dentin. As the resin was incapable of penetrating~~ into the water-rich network of fibril collagen, leading to hydrolytic degradation of the water-rich, resin sparse collagen matrix ~~occurred~~

at the bottom of the hybrid layer [23][24]. Moreover, Bis-GMA contains hydrolysis-prone ester functional groups that can undergo degradation over time in aqueous solution. ~~Plasticization of the polymerized resinous~~ This might have also contributed to the degradation of resin-dentin bonds [23,25]. ~~The HEMA monomer probably reduced the amount of Zr-Ca complexes bound to demineralized dentin after bonding [26]~~.

However, there are certain limitations in the present study. Long-term aging studies, both *in vitro* and *in vivo* are needed to confirm the obtained results, before the zirconium oxynitrate etchant can be widely recommended as an alternative to conventional $H_3PO_4$ etching. Moreover, in the present research, no information is given on the micro-structural changes in the dentin substrate after etching with the experimental material. Ongoing research on the matter should provide additional information on the mechanism and etching ability of the tested material.

## 5. Conclusions

The experimental zirconium oxynitrate etchant has the ability to inhibit dentin endogenous enzymes and improve bond strength, particularly when used before a universal adhesive containing functional monomers. Hence, ZON could be a promising new etching system for various clinical situations, that could overcome some of the drawbacks of the traditional phosphoric acid etchants. ~~Within the limits of the present *in vitro* study, it may be concluded that the experimental zirconium oxynitrate etchant has the ability of inhibiting dentin endogenous enzymes. This etchant has the potential to preserve the integrity of the hybrid layer when universal adhesives are used in the etch-and-rinse mode. Long-term aging studies are required to confirm the results obtained from *in situ* zymography before the zirconium oxynitrate etchant can be recommended as an alternative to conventional $H_3PO_4$ etching.~~

**References**


[1] B. Van Meerbeek, K. Yoshihara, Y. Yoshida, A. Mine, J. De Munck, K.L. Van Landuyt, State of the art of self-etch adhesives, Dent. Mater. 27 (2011) 17–28. doi:10.1016/j.dental.2010.10.023.

[2] D.H. Pashley, F.R. Tay, L. Breschi, L. Tjäderhane, R.M. Carvalho, M. Carrilho, A. Tezvergil-Mutluay, State of the art etch-and-rinse adhesives, Dent. Mater. 27 (2011) 1–16. doi:10.1016/j.dental.2010.10.016.

[3] L. Breschi, T. Maravic, S.R. Cunha, A. Comba, M. Cadenaro, L. Tjäderhane, D.H. Pashley, F.R. Tay, A. Mazzoni, Dentin bonding systems: From dentin collagen structure to bond preservation and clinical applications, Dent. Mater. 34 (2018) 78–96. doi:10.1016/j.dental.2017.11.005.

[4] L. Breschi, A. Mazzoni, A. Ruggeri, M. Cadenaro, R. Di Lenarda, E. De Stefano Dorigo, Dental adhesion review: Aging and stability of the bonded interface, Dent. Mater. 24 (2008) 90–101. doi:10.1016/j.dental.2007.02.009.

[5] A. Abu-Hanna, V. V. Gordan, I. Mjor, The effect of variation in etching times on dentin bonding, Gen. Dent. 52 (2004) 28–33.

[6] M. Hashimoto, H. Ohno, M. Kaga, H. Sano, F.R. Tay, H. Oguchi, Y. Araki, M. Kubota, Over-etching effects on micro-tensile bond strength and failure patterns for two dentin bonding systems, J. Dent. 30 (2002) 99–105. doi:10.1016/S0300-5712(02)00004-0.

[7] A. Mazzoni, D.H. Pashley, Y. Nishitani, L. Breschi, F. Mannello, L. Tjäderhane, M. Toledano, E.L. Pashley, F.R. Tay, Reactivation of inactivated endogenous proteolytic activities in phosphoric acid-etched dentine by etch-and-rinse adhesives, Biomaterials. 27 (2006) 4470–4476. doi:10.1016/j.biomaterials.2006.01.040.

[8] Y. Nishitani, M. Yoshiyama, B. Wadgaonkar, L. Breschi, F. Mannello, A. Mazzoni, R.M. Carvalho, L. Tjäderhane, F.R. Tay, D.H. Pashley, Activation of gelatinolytic/collagenolytic activity in dentin by self-etching adhesives., Eur. J. Oral Sci. 114 (2006) 160–6. doi:10.1111/j.1600-0722.2006.00342.x.

[9] D. Pashley, F. Tay, C. Yiu, M. Hashimoto, L. Breschi, R. Carvalho, Collagen degradation by host-derived enzymes during aging, J. Dent. Res. 83 (2004) 216–221.

[10] A. Almahdy, G. Koller, S. Sauro, J.W. Bartsch, M. Sherriff, T.F. Watson, A. Banerjee, Effects of MMP Inhibitors Incorporated within Dental Adhesives, J. Dent. Res. 91 (2012) 605–611. doi:10.1177/0022034512446339.

[11] C. Yao, M.H. Ahmed, K. Yoshihara, B. Mercelis, C. Parise Gré, K.L. Van Landuyt, C. Huang, B. Van Meerbeek, Bonding to enamel using alternative Enamel Conditioner/etchants, Dent. Mater. 35 (2019) 1415–1429. doi:10.1016/j.dental.2019.07.022.

[12] J. Camilleri, A. Cutajar, B. Mallia, Hydration characteristics of zirconium oxide replaced Portland cement for use as a root-end filling material, Dent. Mater. 27 (2011) 845–854. doi:10.1016/j.dental.2011.04.011.

[13] F.R. Tay, D.H. Pashley, M. Yoshiyama, Two modes of nanoleakage expression in single-step adhesives, J Dent Res. 81 (2002) 472–476. doi:10.1177/154405910208100708.

[14] V. Saboia, F. Nato, A. Mazzoni, G. Orsini, A. Putignano, M. Giannini, Adhesion of a two-step etch-and-rinse adhesive on collagen-depleted dentin, J. Adhes. Dent. 10 (2008).

[15] A. Mazzoni, P. Scaffa, M. Carrilho, L. Tjäderhane, R. Di Lenarda, A. Polimeni, A. Tezvergil-Mutluay, F.R. Tay, D.H. Pashley, L. Breschi, Effects of etch-and-rinse and self-etch adhesives on dentin MMP-2 and MMP-9., J. Dent. Res. 92 (2013) 82–86. doi:10.1177/0022034512467034.

[16] A. Comba, N. Scotti, A. Mazzoni, T. Maravic, S. Ribeiro Cunha, R. Michelotto Tempesta, M. Carossa, D.H. Pashley, F.R. Tay, L. Breschi, Carbodiimide inactivation of matrix metalloproteinases in radicular dentine, J. Dent. 82 (2019) 56–62. doi:10.1016/j.jdent.2019.01.007.

[17] A.S. Solovkin, Z.N. Tsvetkova, THE CHEMISTRY OF AQUEOUS SOLUTIONS OF ZIRCONIUM SALTS (DOES THE ZIRCONYL ION EXIST?), Russ. Chem. Rev. 31 (1962) 655–669. doi:10.1070/rc1962v031n11abeh001326.

[18] M.C.G. Erhardt, J. Pisani-Proença, E. Osorio, F.S. Aguilera, M. Toledano, R. Osorio, Influence of laboratory degradation methods and bonding application parameters on microTBS of self-etch adhesives to dentin., Am. J. Dent. 24 (2011) 103–108.

[19] R. Visse, H. Nagase, Matrix metalloproteinases and tissue inhibitors of metalloproteinases: Structure, function, and biochemistry, Circ. Res. 92 (2003) 827–839. doi:10.1161/01.RES.0000070112.80711.3D.

[20] S. Sauro, F. Mannocci, M. Toledano, R. Osorio, D.H. Pashley, T.F. Watson, EDTA or H3PO4/NaOCl dentine treatments may increase hybrid layers' resistance to degradation: A microtensile bond strength and confocal-micropermeability study, J. Dent. 37 (2009) 279–288. doi:10.1016/j.jdent.2008.12.002.

[21] H. Nurrohman, T. Nikaido, T. Takagaki, A. Sadr, S. Ichinose, J. Tagami, Apatite crystal protection against acid-attack beneath resin-dentin interface with four adhesives: TEM and crystallography evidence, Dent. Mater. 28 (2012). doi:10.1016/j.dental.2012.04.025.

[22] Y. Yoshida, K. Yoshihara, N. Nagaoka, S. Hayakawa, Y. Torii, T. Ogawa, A. Osaka, B. Van Meerbeek, Self-assembled Nano-layering at the Adhesive interface., J. Dent. Res. 91 (2012) 376–81. doi:10.1177/0022034512437375.

[23] P.D. Tay FR, King NM, Chan K, How can nanoleakage occur in self-etching adhesive

systems that demineralize and infiltrate simultaneously? | Request PDF, J Adhes Dent. (2002) 4: 255-269.

[24] M. Hanabusa, A. Mine, T. Kuboki, Y. Momoi, A. Van Ende, B. Van Meerbeek, J. De Munck, Bonding effectiveness of a new "multi-mode" adhesive to enamel and dentine, J. Dent. 40 (2012) 475–484. doi:10.1016/j.jdent.2012.02.012.

[25] P.J. Koin, A. Kilislioglu, M. Zhou, J.L. Drummond, L. Hanley, Analysis of the degradation of a model dental composite, J. Dent. Res. 87 (2008) 661–665. doi:10.1177/154405910808700712.

[26] J. Kim, L. Gu, L. Breschi, L. Tjäderhane, K.K. Choi, D.H. Pashley, F.R. Tay, Implication of ethanol wet-bonding in hybrid layer remineralization, J. Dent. Res. 89 (2010) 575–580. doi:10.1177/0022034510363380.

**Figure legends**

**Figure 1.** Percentage of interfacial nanoleakage expression in resin-dentin interfaces created among the different groups, at $T_0$ and $T_{12}$.

**Figure 2.** Representative light microscopy images (20x magnification) of the tested materials in the experimental conditions and submitted to nanoleakage with silver nitrate after 24 h of storage in artificial saliva ($T_0$). D = Dentin; HL = Hybrid Layer; C = Composite. Arrows indicate areas of silver nitrate particles deposition.

**Figure 3.** Representative light microscopy images (20x magnification) of the tested materials in the experimental conditions and submitted to nanoleakage with silver nitrate after 12 months of storage in artificial saliva ($T_{12}$). D = Dentin; HL = Hybrid Layer; C = Composite. Arrows indicate areas of silver nitrate particles deposition.

**Figure 4.** a) Zymographic analysis of proteins extracted from dentin powder. L1: Standards (STD); L2: mineralized dentin (MIN) showing the presence of activity of pro-form of MMP-9 (92 kDa) and active form of MMP- 2 (66 kDa); L3: demineralized dentin powder (DDP) showing an increase of MMP-9 (86 kDa) and the higher activity of the active form of MMP-2 (66 kDa); L4: Dentin powder demineralized with ZON showing inhibition of MMP-9 and MMP-2 activity. b) Graph illustrating the densitometric evaluation of bands obtained from the zymographic analysis of proteins extracted from dentin powder.

**Figure 5.** Resin-bonded mid-coronal dentin interfaces prepared with ZON/AU (a and e), TE/AU (b and f), ZON/EF (c and g) and TE/EF (d and h) at $T_0$ , incubated with quenched fluorescein-labeled gelatin. (a) Image acquired in green channel, showing fluorescence (identifying intense endogenous enzymatic activity) in dentinal tubules and within the HL created with ZON/AU; (b) Image acquired in green channel, showing fluorescence in dentinal tubules and within the HL created with TE/AU; (c) Image acquired in green channel, showing fluorescence in dentinal tubules and within the HL

created with ZON/EF; (d) Image acquired in green channel, showing fluorescence in dentinal tubules and within the HL created with TE/EF; (e) Image of the HL created by the application of ZON/AU obtained by merging differential interference contrast image (showing the optical density of the resin-dentin interface) and image acquired in green channel; (f) Image of the HL created by the application of TE/AU obtained by merging differential interference contrast image and image acquired in green channel; (g) Image of the HL created by the application of ZON/EF obtained by merging differential interference contrast image and image acquired in green channel; (h) Image of the HL created by the application of TE/EF obtained by merging differential interference contrast image and image acquired in green channel. D = Dentin; HL = Hybrid Layer; R = Resin Composite.

**Figure 6.** Resin-bonded mid-coronal dentin interfaces prepared with ZON/AU (a,e), TE/AU (b,f), ZON/EF (c,g) and TE/EF (d,h) at $T_{12}$, incubated with quenched fluorescein-labeled gelatin. (a) Image acquired in green channel, showing fluorescence (identifying intense endogenous enzymatic activity) in dentinal tubules and within the HL created with ZON/AU; (b) Image acquired in green channel, showing fluorescence in dentinal tubules and within the HL created with TE/AU; (c) Image acquired in green channel, showing fluorescence in dentinal tubules and within the HL created with ZON/EF; (d) Image acquired in green channel, showing fluorescence in dentinal tubules and within the HL created with TE/EF; (e) Image of the HL created by the application of ZON/AU obtained by merging differential interference contrast image (showing the optical density of the resin-dentin interface) and image acquired in green channel; (f) Image of the HL created by the application of TE/AU obtained by merging differential interference contrast image and image acquired in green channel; (g) Image of the HL created by the application of ZON/EF obtained by merging differential interference contrast image and image acquired in green channel; (h) Image of the HL created by the application of TE/EF obtained by merging differential interference contrast image and image acquired in green channel. D = Dentin; HL = Hybrid Layer; R = Resin Composite.

**Figure 7**. *In situ* zymography quantification at $T_0$ and $T_{12}$ showing reduced enzymatic activity in ZON groups when used in association with both AU and EF adhesive systems.

## TABLES

**Table 1.** Chemical composition of the materials used in the study and bonding procedures.

| Material | Composition | pH | Bonding procedures |
|---|---|---|---|
| **Adhese Universal**<br>Ivoclar Vivadent Schaan Liechtenstein | MDP, MCAP, HEMA, Bis-GMA, D3MA, water, ethanol, highly dispersed silica, catalysts, initiators and stabilizers | 2.5- 3 | 1. After acid etching, apply adhesive on dentin and agitate for at least 20 s;<br>2. Air-spray with oil- and moisture-free compressed air until a glossy, immobile film is obtained;<br>3. Light-cure using a LED light-curing unit for 20 s. |
| **Excite F**<br>Ivoclar Vivadent | Phosphonic acid acrylate, HEMA, D3MA, ethanol, highly dispersed silica, catalysts, initiator and stabilizers, fluoride | 2.5 | 1. After acid etching, apply adhesive on dentin and agitate for at least 10 s;<br>2. Thin the adhesive with an oil- and moisture-free compressed air until a glossy, immobile film is obtained;<br>3. Light-cure using a LED light-curing unit for 20 s. |
| **Experimental etchant (ZON)**<br>Ivoclar Vivadent | $ZrO(NO_3)_2$, water, glycerol, fumed silica, polyethylene oxide | 0.56 | 1. Apply ZON and allow it to interact with the tooth surface without agitation for 30 s;<br>2. Thoroughly rinse off the etchant with water spray and dry with oil-free air;<br>3. Continue with bonding procedures. |
| **Total Etch**<br>Ivoclar Vivadent | Phosphoric acid (37 wt% in water), thickening agent and color pigments | 0,1-0,4 | 1. Apply the etchant and allow it to interact with the tooth surface without agitation for 15 s;<br>2. Thoroughly rinse off the etchant with water spray and dry with oil-free air.<br>3. Continue with bonding procedures. |

**Abbreviations**: Bis-GMA - bisphenol A-glycidyl methacrylate; D3MA - decandiol dimethacrylate; HEMA – 2-hydroxyethyl methacrylate; LED – light emitting diode; MCAP - methacrylated carboxylic acid polymer; MDP - methacryloyloxydecyl dihydrogen phosphate

**Table 2.** Summary of microtensile bond strength results obtained from the four experimental groups immediately ($T_0$) and after 12 months of laboratory aging ($T_{12}$).

| Etchant/Adhesive | $T_0$ (MPa) † | $T_{12}$ (MPa) † |
|---|---|---|
| **ZON/AU** | 54.3 ± 15.0 $^{a,A}$ | 43.9 ± 14.2 $^{a,B}$ |
| **TE/AU** | 39.1 ± 14.2 $^{b,A}$ | 36.0 ± 14.1 $^{a,b,A}$ |
| **ZON/EF** | 42.1 ± 17.9 $^{b,A}$ | 26.9 ± 14.3 $^{b,c,B}$ |
| **TE/EF** | 37.9 ± 16.2 $^{b,A}$ | 20.8 ± 14.8 $^{c,B}$ |

† Values are means ± standard deviations, in megaPascals (MPa).

Abbreviations: ZON - experimental zirconia oxynitrate [$ZrO(NO_3)_2$] etchant; TE - Total Etch conventional 37% phosphoric acid ($H_3PO_4$) etchant; AU - universal adhesive Adhese Universal; EF - 2-step self-etch adhesive Excite F.

Different lower-case letters indicate significant differences within the same column ($p < 0.05$),

Different upper-case letters indicate significant differences within the same row ($p < 0.05$).

**Table 3.** Failure mode distributions and their percentages identified from the four experimental groups after bond strength testing at $T_0$ and $T_{12}$.

| | Failure mode (%) | | | | | | | |
|---|---|---|---|---|---|---|---|---|
| | $T_0$ | | | | $T_{12}$ | | | |
| | **A** | **CC** | **CD** | **M** | **A** | **CC** | **CD** | **M** |
| **ZON/AU** | 43% | 34% | 0% | 23% | 19% | 73% | 6% | 2% |
| **TE/AU** | 28% | 43% | 6% | 24% | 24% | 61% | 11% | 4% |
| **ZON/EF** | 57% | 22% | 2% | 20% | 81% | 11% | 3% | 5% |
| **TE/EF** | 47% | 21% | 8% | 25% | 52% | 32% | 0% | 16% |

Failure modes: A - adhesive; CC - cohesive in composite; CD - cohesive in dentin; M – mixed

Abbreviations: ZON - experimental $ZrO(NO_3)_2$ etchant; TE - Total Etch 37% $H_3PO_3$; AU - Adhese Universal adhesive; EF - Excite F adhesive

Figure 1. Percentage of interfacial nanoleakage expression (T0 and T12)

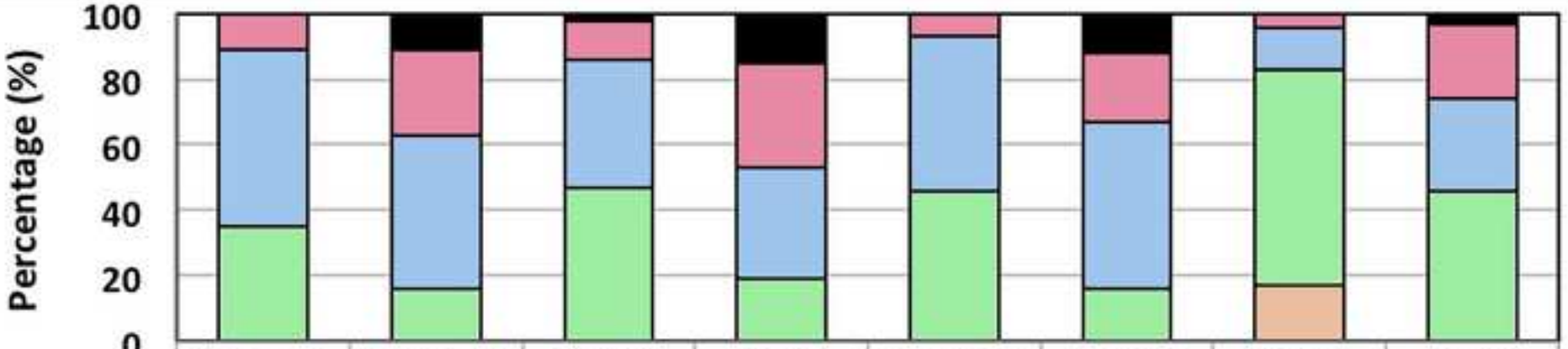


| | ZON/AU $T_0$ | ZON/AU $T_{12}$ | TE/AU $T_0$ | TE/AU $T_{12}$ | ZON/EF $T_0$ | ZON/EF $T_{12}$ | TE/EF $T_0$ | TE/EF $T_{12}$ |
|---|---|---|---|---|---|---|---|---|
| > 75 | 0 | 11 | 2 | 15 | 0 | 12 | 0 | 3 |
| 50 ≤ 75 | 11 | 26 | 12 | 32 | 7 | 21 | 4 | 23 |
| 25 ≤ 50 | 54 | 47 | 39 | 34 | 47 | 51 | 13 | 28 |
| < 25 | 35 | 16 | 47 | 19 | 46 | 16 | 66 | 46 |
| 0 | 0 | 0 | 0 | 0 | 0 | 0 | 17 | 0 |

Figure 2. Light microscopy images of nanoleakage at T0

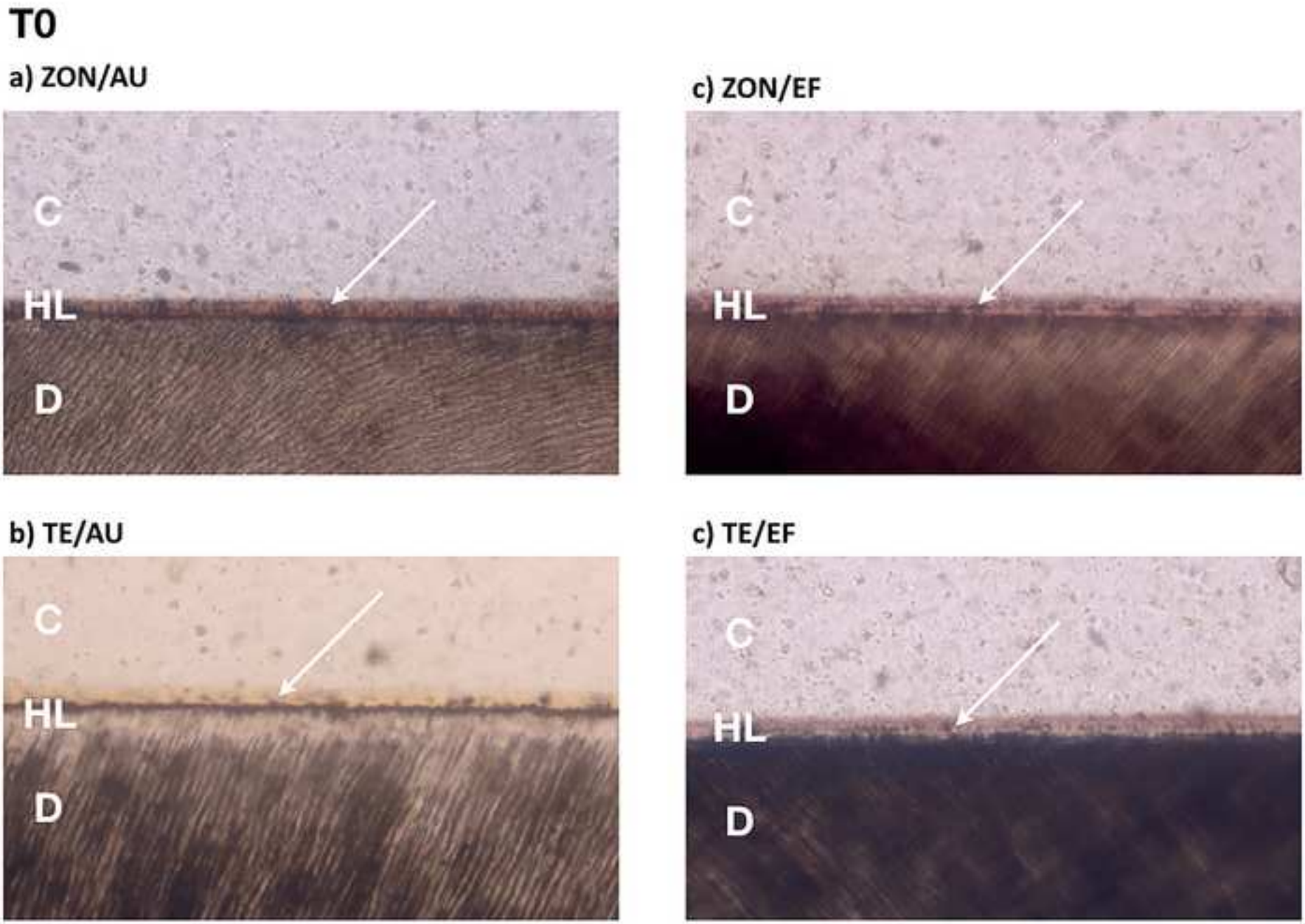

Figure 3. Light microscopy images of nanoleakage at T12

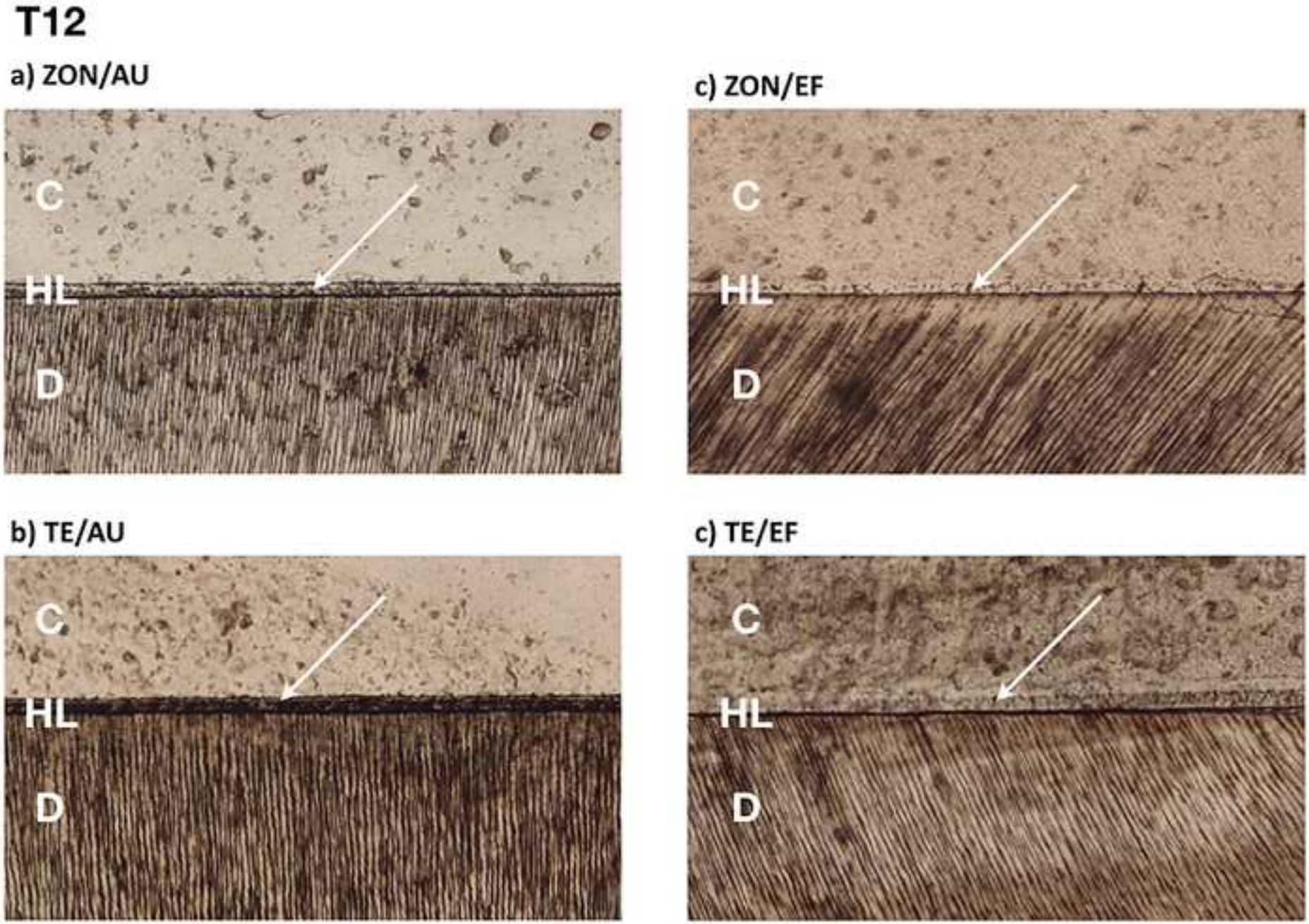

Figure 4. Zymographic analysis of proteins extracted from dentin powder.

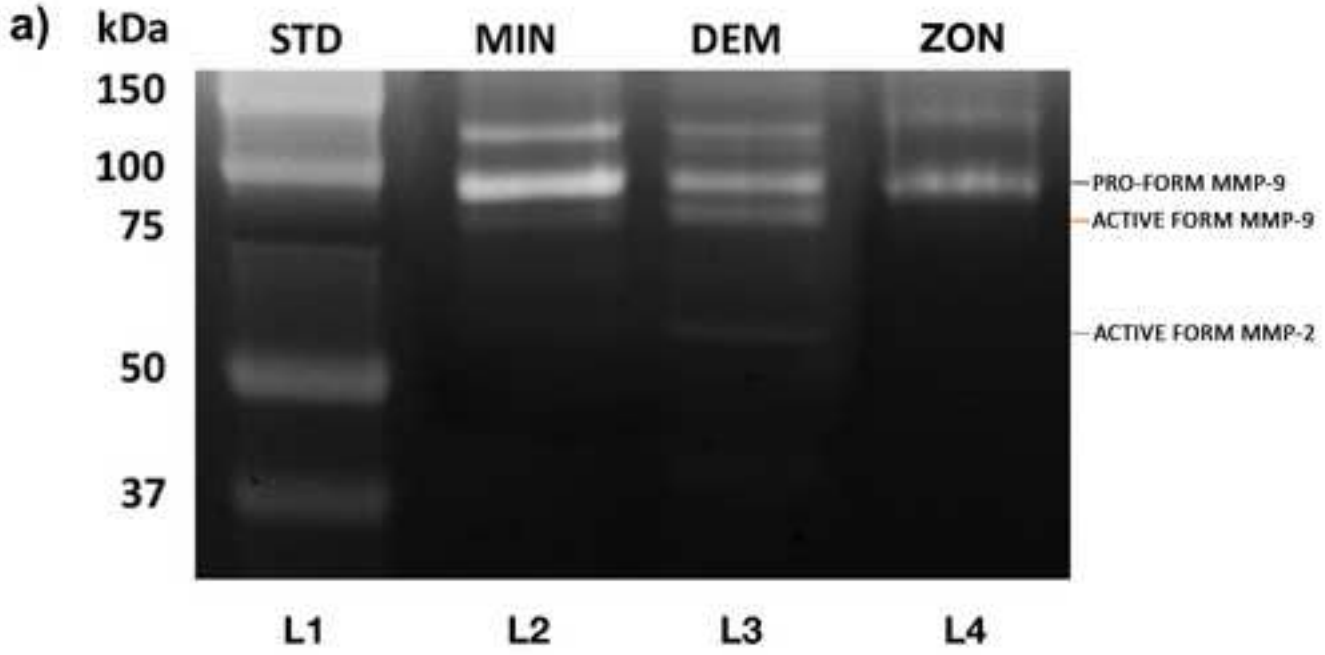


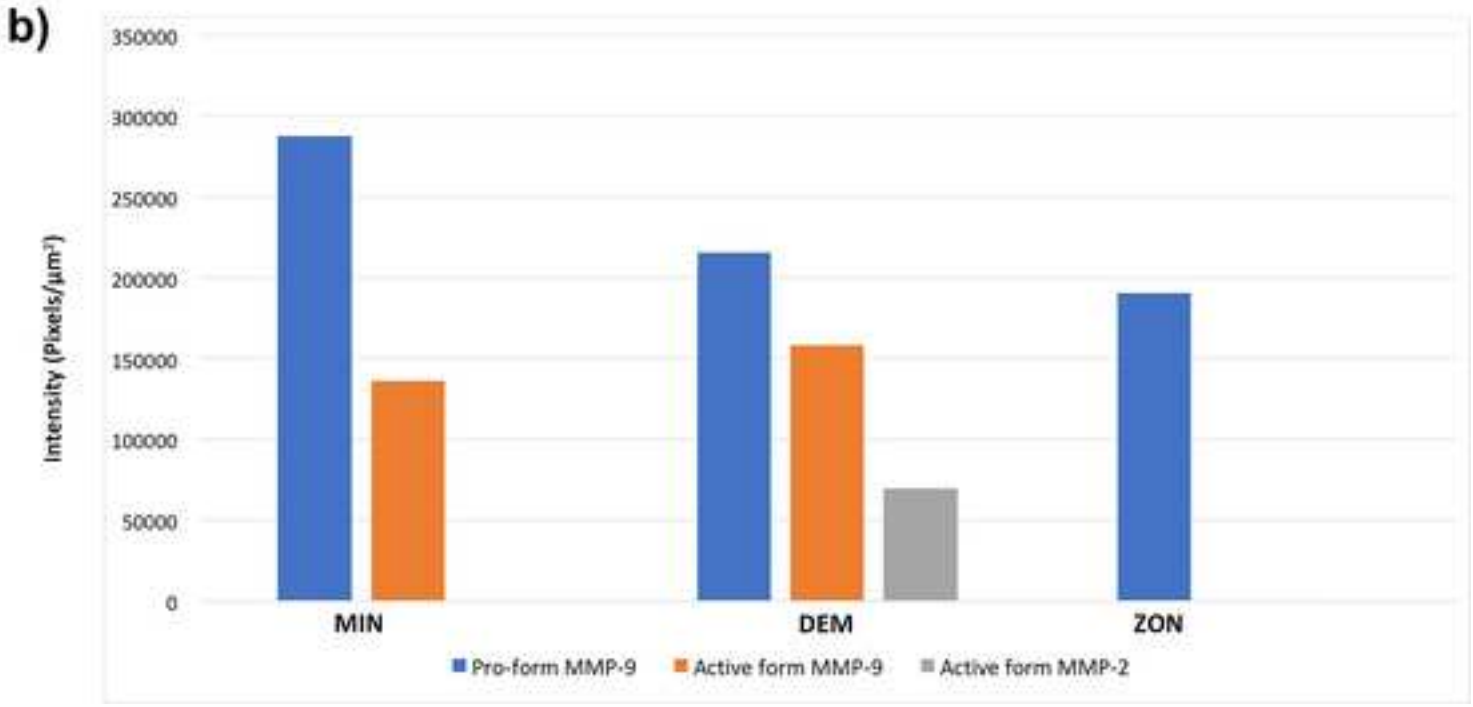

Figure 5. In situ zymography (T0).

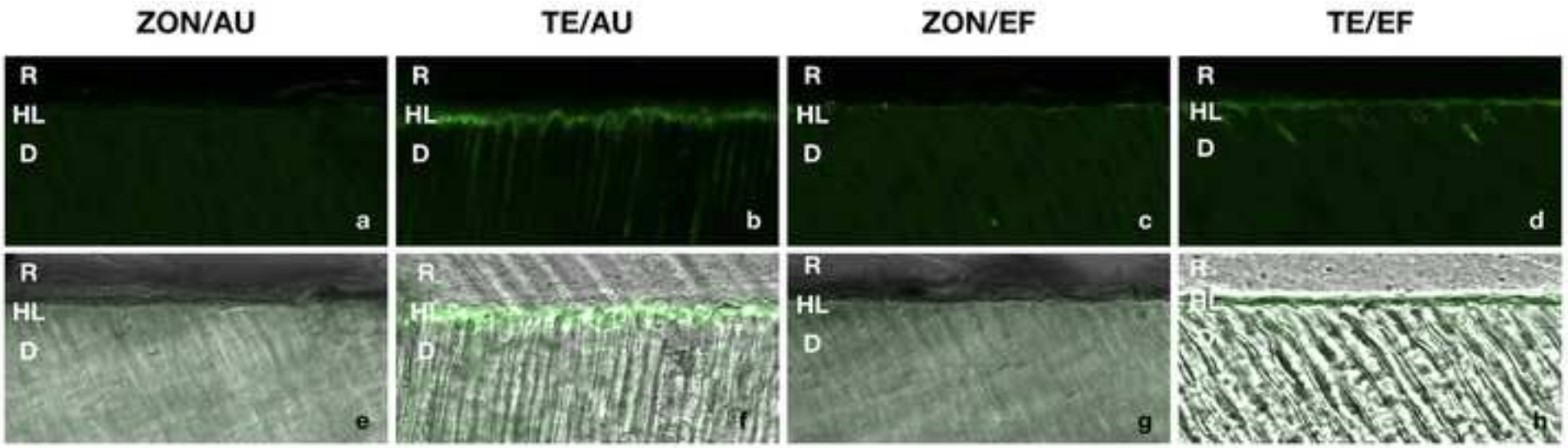

Figure 6. In situ zymography (T12).

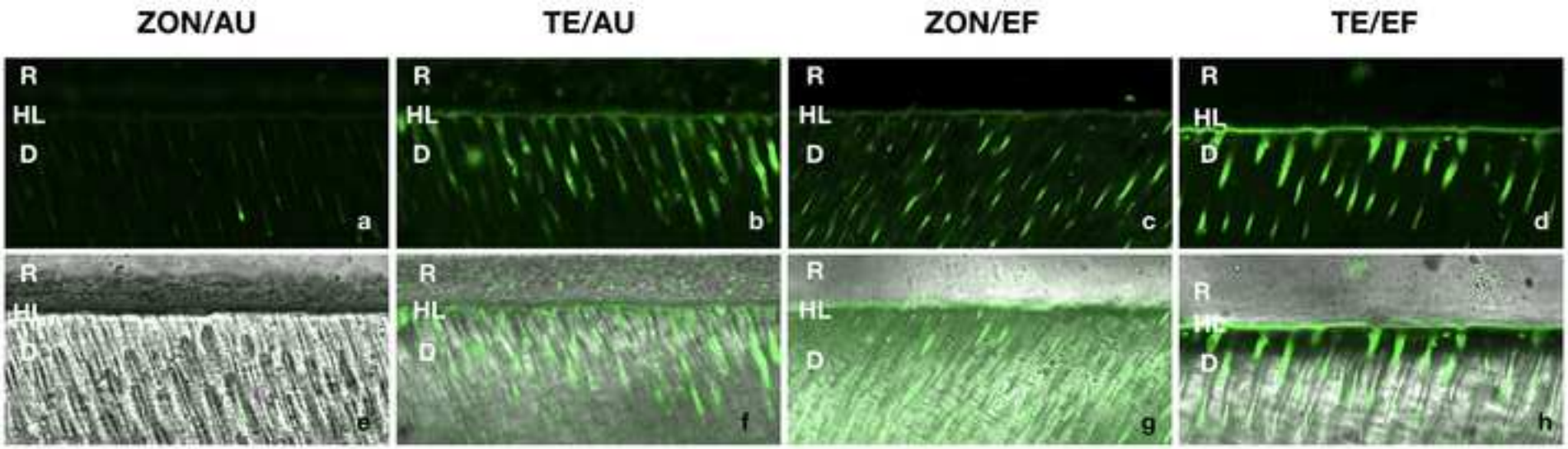

Figure 7. In situ zymography quantification.

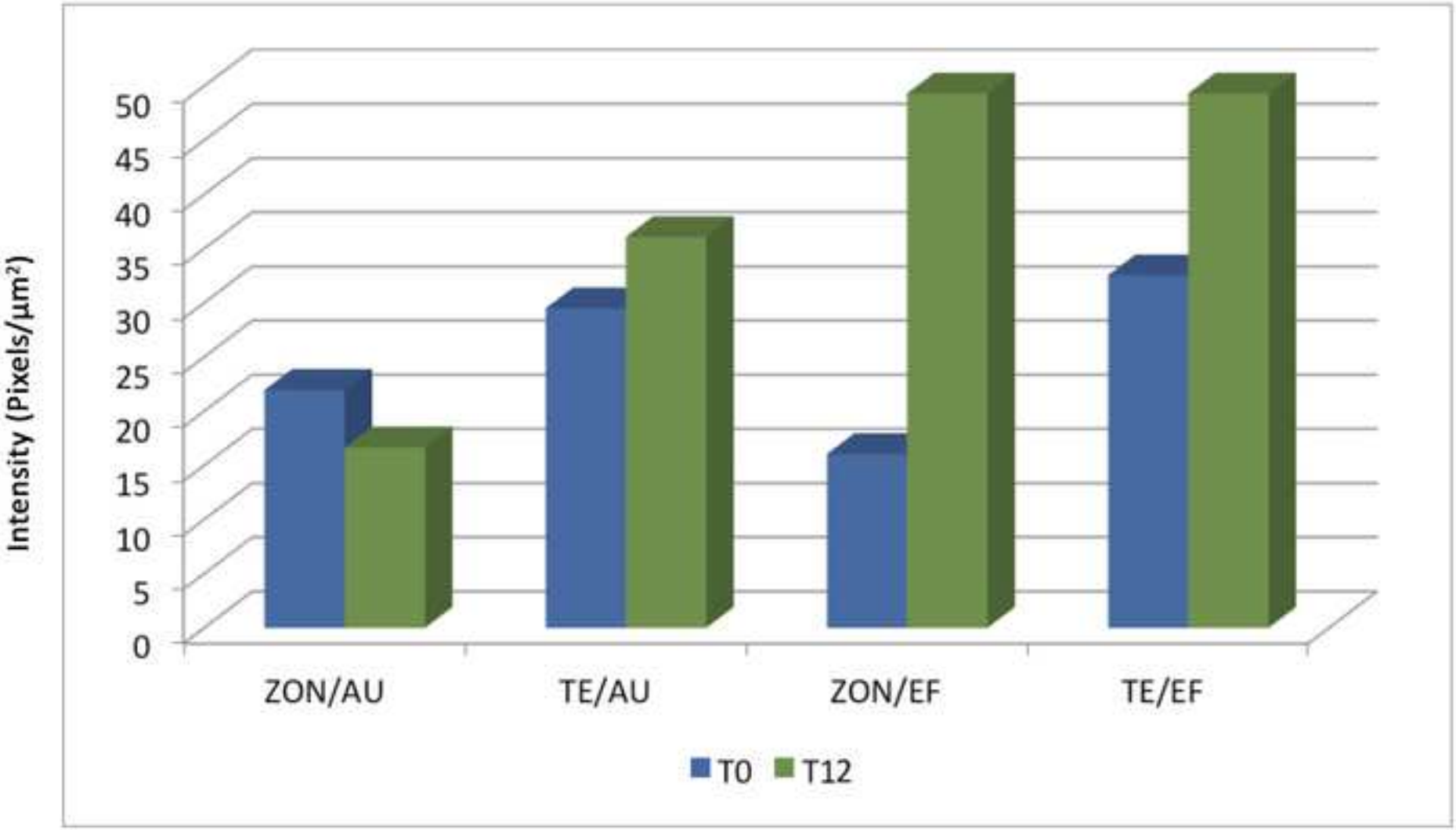

**Credit authors statement**

**Edoardo Mancuso:** investigation, visualization, writing—original draft preparation**; Allegra Comba:** formal analysis, writing—original draft preparation; **Claudia Mazzitelli:** data curation, writing—review and editing**; Tatjana Maravic:** investigation, writing—review and editing; **Uros Josic:** visualization, writing—review and editing; **Federico Del Bianco:** validation, writing—original draft preparation; **Franklin R Tay:** formal analysis, methodology, writing— review and editing; **Lorenzo Breschi:** project administration, funding acquisition, writing—review and editing; **Annalisa Mazzoni:** conceptualization, methodology, supervision, writing—review and editing. All authors have read and approved the final version of the manuscript.